TOWARDS REALISTIC FLOW MODELLING. CREATION AND EVALUATION OF TWO-DIMENSIONAL SIMULATED POROUS MEDIA: AN IMAGE ANALYSIS APPROACH

YANNICK ANGUY[1], DOMINIQUE BERNARD[1] and ROBERT EHRLICH[2]
[1]*Laboratoire Energétique et Phénomènes de Transfert, U.R.A.-CNRS No. 873, Ecole Nationale Supérieure des Arts et Métiers, 33405 Talence Cedex, France;* [2]*Department of Geological Sciences, University of South Carolina, Columbia, S. C., 29208, USA*

Abstract. This work is part of an attempt to quantify the relationship between the permeability tensor (**K**) and the micro-structure of natural porous media. A brief account is first provided of popular theories used to relate the micro-structure to **K**. Reasons for the lack of predictive power and restricted generality of current models are discussed. An alternative is an empirically based implicit model wherein **K** is expressed as a consequence of a few "pore-types" arising from the dynamics of depositional processes. The analytical form of that implicit model arises from evidence of universal association between pore-type and throat size in sandstones and carbonates. An explicit model, relying on the local change of scale technique is then addressed. That explicit model allows, from knowledge of the three-dimensional micro-geometry to calculate **K** explicitly without having recourse to any constitutive assumptions. The predictive and general character of the explicit model is underlined. The relevance of the change of scale technique is recalled to be contingent on the availability of rock-like three-dimensional synthetic media. A random stationary ergodic process is developed, that allows us to generate three-dimensional synthetic media from a two-dimensional autocorrelation function $r(\lambda_x, \lambda_y)$ and associated probability density function ϵ_β measured on a single binary image. The focus of this work is to ensure the rock-like character of those synthetic media. This is done first through a direct approach: n two-dimensional synthetic media, derived from single set $(\epsilon_\beta, r(\lambda_x, \lambda_y))$ yield n permeability tensors $\mathbf{K}^i_{i=1,n}$ (calculated by the local change of scale) of the same order. This is a necessary condition to ensure that $r(\lambda_x, \lambda_y)$ and ϵ_β carry all structural information relevant to **K**. The limits of this direct approach, in terms of required Central Process Unit time and Memory is underlined, raising the need for an alternative. This is done by comparing the pore-type content of a sandstone sample and n synthetic media derived from $r(\lambda_x, \lambda_y)$ and ϵ_β measured on that sandstone-sample. Achievement of a good match ensures that the synthetic media comprise the fundamental structural level of all natural sandstones, that is a domainal structure of well-packed clusters of grains bounded by loose-packed pores.

Key words: Local change of scale, permeability tensor, local Representative Elementary Volume, image analysis, pore-types, random stationary ergodic process, Fourier transforms, micro-structure

Nomenclature

C_k	adjustable parameter
d_j	diameter of the throats associated to the pores of the jth type (m)
$\lvert F_e(\nu_x, \nu_y)\rvert^2$	squared Fourier modulus of the Fourier transform (subscript e indicates that the micro-geometry has been 0-appended).
$F(\nu_x, \nu_y)$	Fourier modulus of the Fourier transform
$\mathcal{F}$	formation factor
k	scalar component of Darcy's law permeability tensor (m^2, 1 darcy $\cong 10^{-12}$ m^2)

Surveys in Geophysics **17:** 265–287, 1996.

$\mathbf{K}$	Darcy's law permeability tensor (m^2, 1 darcy $\cong 10^{-12}$ m^2)
l_c	threshold length from mercury injection (m)
L_c	length-scale at which the micro-structure is no longer correlated
l_β	mean pore size (m)
l_σ	mean grain size (m)
Np_j	number of pores of the jth type per μm^2
P_c	capillary pressure (N/m^2)
r_0	characteristic length-scale of the local geometrical Representative Elementary Volume (m)
r_0	characteristic length-scale of the local Darcy's Representative Elementary Volume (m)
$r(\lambda_x, \lambda_y)$	2-D autocorrelation function
$V_\beta(r_0)$	local geometrical Representative Elementary Volume (m^3)
$V_\beta(r_0)$	local averaging volume of Darcy's type (m^3)
(λ_x, λ_y)	2-D spatial wave-length expressed in a local Cartesian basis (m)
(ν_x, ν_y)	2-D spatial wave-number expressed in a local Cartesian basis
$\varphi(\nu_x, \nu_y)$	complete phase of the Fourier transform
$\zeta(\nu_x, \nu_y)$	part of the phase of the Fourier transform
ϵ_β	volume fraction of the void phase (porosity)

1. Introduction

This work is part of an ongoing effort to link the micro-geometry of natural media to the permeability tensor $\mathbf{K}$. Quantifying the dependence of $\mathbf{K}$ on the micro-structure of natural media is of prime importance in many fields such as exploration and production in oil industry, enhanced petroleum recovery, and contaminated ground-water remediation. The dependence of $\mathbf{K}$ on the micro-structure has been acknowledged in a number of ways, either empirically (Dullien, 1979) or theoretically (Anguy *et al.*, 1994a; Whitaker, 1986). Whatever the model, the thing is to express into a predictive and analytical model that $\mathbf{K}$ is an implicit function of the micro-structure (relation 1), so that a micro-structural change yields a variation $\mathrm{d}\mathbf{K}$ of $\mathbf{K}$.

$$\mathbf{K} = f\,(\text{micro-structure}) \tag{1}$$

Models dealt with in the literature differ essentially in the structural parameters $P^i_{i=1,N'}$ held to formulate implicit relation 1 into a predictive model (relations 2 to 4):

$$\text{micro-structure} = f(P^i_{i=1,N}) \tag{2}$$

$$\mathbf{K} = g(P^i_{i=1,N'})_{N' \leq N} \tag{3}$$

$$\mathrm{d}\mathbf{K} = \sum_{i=1}^{N'} \frac{\partial g}{\partial P^i} \mathrm{d}P^i \tag{4}$$

where the micro-structure is characterized, through an implicit function f, by N geometrical parameters measurable by experiment $(P^i_{i=1,N})$. **K** is characterized, through an implicit function g, by that minimal **K**-relevant subset, $P^i_{i=1,N',N'\leq N}$, included in set $P^i_{i=1,N}$ and $\sum_{i=1}^{N'} \partial g/\partial P^i$ is an intrinsic function of the model used to derive **K**.

The appropriate **K**-relevant $P^i_{i=1,N'}$ are not known a-priori, whence the diversity of models. There is a general agreement that **K** does not arise solely from porosity, ϵ_β: *"It is obvious that no simple correlation between porosity and permeability can exist"* (Scheidegger, 1974). The micro-structure must be characterized more completely by a set of parameters $P^i_{i=1,N}$ accounting for the spatial arrangement of porosity. Attempts to relate **K** to the sole parameter $P^1 = \epsilon_\beta$ met with tangible success in cases where the structural variability among the samples was strictly linked to ϵ_β (relations 5):

$$P^1 = \epsilon_\beta,\ (\mathrm{d}P^i = h^i(P^1))_{i=2,N'} \tag{5}$$

where $h^i_{i=2,N'}$ are implicit functions. Correlations between **K** and ϵ_β are limited to samples verifying the same relations $h^i_{i=2,N'}$. Consequently, correlations between **K** and ϵ_β representative of the present state of a reservoir might be totally inappropriate to simulate its diagenetic history.

The models dealt with in the literature might be classified with respect to two extreme cases: the implicit and the explicit models.

In implicit models, the direct characterization of the micro-geometry (relation 2) is commonly by-passed. Instead, fundamental laws (for example, Washburn equation) are introduced in experimental results to quantify **K**-relevant *effective* structural parameters $Q^j_{j=1,\mathcal{M}}$. That is:

$$k = \hbar(Q^j_{j=1,\mathcal{M}}) \tag{6}$$

where $\hbar$ is an implicit function and k, a scalar component of **K**.

Implicit relation (6) is then formulated as an analytical model arising from various physical and/or geometrical bases. Work by Ehrlich *et al.* (1991a) and McCreesh *et al.* (1991) yields as $Q^j_{j=1,\mathcal{M}}$ $\mathcal{M}$ geometrical parameters $Np_{j,j=1,\mathcal{M}}$ (obtained by petrographic image analysis producing a pore-type base for porosity classification) and $\mathcal{M}$ physical parameters $d_{j,j=1,\mathcal{M}}$ (obtained combining image analysis data, e.g. pore-types, with mercury drainage experiments) (Equation (7)):

$$(Q^j)_{j=1,\mathcal{M}} = (Np_j, d_j)_{j=1,\mathcal{M}} \tag{7}$$

where d_j is the diameter of the throats associated with the pores of the jth pore-type, and Np_j is the number of pores of the jth pore-type per $\mu\mathrm{m}^2$.

Relations (6) and (7) yield:

$$k = \hbar(Np_j, d_j)_{j=1,\mathcal{M}} \tag{8}$$

In Ehrlich *et al.* (1991b), implicit relation (8) is then worked out in an analytical tube-like model (Equation (9)) relying on the association between pore-type and throat size (C_k is an adjustable parameter).

$$k = 1013\, C_k \sum_{j=1}^{\mathcal{M}} \frac{N p_j \pi d_j^4}{128} \tag{9}$$

Relation (6) differs from relation (3) in that, part of the geometrical information is integrated by the experimental process used to quantify the effective parameters $Q^j_{j=1,\mathcal{M}}$. That point is as expressed by Equation (10). That is, the $Q^j_{j=1,\mathcal{M}}$ are related to an effective medium.

$$(Q^j)_{j=1,\mathcal{M}} = \mathcal{L}((P^i)_{i=1,N}) \tag{10}$$

where $\mathcal{L}$ is an unknown additional functional of the geometrical parameters $P^i_{i=1,N}$. Generally, this additional functional requires a *"tuning" constant* (C_k in Equation (9)) to formulate the analytical relation linking the $Q^j_{j=1,\mathcal{M}}$ to k. Optimal value of that "tuning" constant can only be estimated by curve-fitting with respect to a set of measured permeabilities ($k_{j,j=1,\mathcal{K}}$) derived from $\mathcal{K}$ samples. As mentioned above (Equation (5)), the predictive character of the model is accordingly limited to samples verifying additional relations $h^i_{i=\mathcal{M}+1,\mathcal{M}+\mathcal{P}}$. That is:

$$(Q^j)_{j=1,\mathcal{M}} = (Np_j, d_j)_{j=1,\mathcal{M}}; (dQ^i = h^i(Q_j)_{j=1,\mathcal{M}})_{i=1,\mathcal{M}+1,\mathcal{M}+\mathcal{P}} \tag{11}$$

The generality of implicit models depends on the generality of the physical and/or geometrical arguments used to formulate the $Q^j_{j=1,\mathcal{M}}$ in an analytical model. Furthermore a predictive model must be able to predict the physical properties of a single sample (Garboczi, 1990).

For percolation models (Equation (12)) (Thompson, 1991) no curve-fitting is required, but the requirement of a *random* distribution of tube radii makes the model inadequate to predict physical properties of sandstones and carbonates due to the universal occurrence of a non-random structure as a consequence of depositional processes (Prince *et al.*, 1995; Anguy *et al.*, 1994b).

$$k = (226)^{-1} l_c^2 \mathcal{F}^{-1} \tag{12}$$

where $\mathcal{F}$ is the formation factor and l_c is a threshold diameter.

A *pure* explicit model is supposed to simulate directly the behaviour of a porous medium. Commonly, the actual micro-structure is simplified through an implicit approach so that explicit-like modelling is two-fold: (1) quantify the structural effective characteristics $Q^j_{j=1,\mathcal{M}}$ of the elements of the model, (2) simulate flow over a network built using those elements (Quiblier, 1984).

The structural characteristics $Q^j_{j=1,\mathcal{M}}$ are assessed as for implicit models (for example, based on mercury intrusion curves (Dullien, 1975)). The structural elements might be cylindrical tubes with circular section (Haring *et al.*, 1970) or

with step-changing diameters (Azam *et al.*, 1977). The elements of characteristics $Q^j_{j=1,\mathcal{M}}$ are then assembled into fixed network that can be, regular (Chatzis *et al.*, 1977) or irregular (Dullien, 1979).

In simulating flow over the network, one intends to derive a new and more general expression for the implicit function h (Equation (6)). That is, an explicit model, *per se*, is of little interest in that, every different porous material has to be measured the same way with no way of predicting k without going through the whole process. Thus, explicit models are worth only as a *step towards* building a better e.g., more general implicit model. Nonetheless, as discussed in Bryant (1993), explicit models are questionable due to common simplifying assumptions fitted in the models (regular lattice, shape of the pores, network coordination number, ...) that yield errors that might cancel each other.

In this work, an "almost" pure explicit approach is developed that aims at overcoming the lack of predictiveness and generality of the models dealt with above. No effective parameters $Q^j_{j=1,\mathcal{M}}$ are used. This is consistent with Bryant (1993) who underlined that "... *void space in a porous media can be properly represented by a graph of connected sites* ..." provided that the network involves no *a priori* simplifications about the micro-structure.

A complete measure of the micro-geometry is proposed in terms of N geometrical parameters $P^i_{i=1,N}$, measurable by image analysis of a single sample. That complete measure is reduced to a minimal K-relevant subset $P^i_{i=1,N',N'\leq N}$ included in the complete set $P^i_{i=1,N}$. The two-dimensional nature of the $P^i_{i=1,N'}$, implied by the experimental process, *image analysis*, used to measure the $P^i_{i=1,N'}$ requires a random stationary ergodic process that allows the generation of a set of n synthetic three-dimensional media from the $P^i_{i=1,N'}$ measured on a single sample. The flow simulation relies on numerical implementation of the local change of scale technique (Anguy *et al.*, 1994a; Anguy, 1993).

The goal of this paper is to ensure whether or not synthetic media derived by a random stationary ergodic process have rock-like structural properties. The problem is addressed in two ways: (1) through a direct approach relying on the local change of scale model, (2) through an indirect approach capitalizing on a model due to Ehrlich (Ehrlich *et al.*, 1991a,b).

2. Implicit Modelling of the Permeability

Characterizing the three-dimensional micro-structure of natural media is complex, current observations being of porosity exposed on two-dimensional thin sections through the medium. Nonetheless, work by Ehrlich (1991a) shows that characteristics observed on sections impose limits on structural variations in the three-dimensional medium.

Porosity, on two-dimensional sections, appears as many discrete patches of porosity, porels (PORosity ELements), identified as closed areas of porosity (Figure

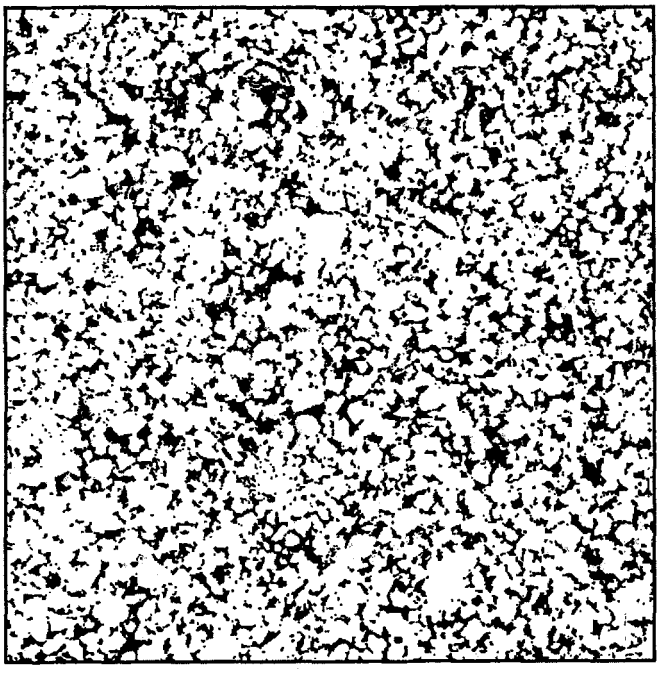

Figure 1. Sample 3 (Perry-Sandstones). Binary mosaic produced 1) by merging high resolution overlapping images (square pixel edge: 3.861 μm) digitized by a colour device and 2) by resampling to obtain a 512 $\times$ 512 pixel image (square pixel edge: 15.44 μm). Mosaic size: 7.905 $\times$ 7.905 mm. Porosity represented by black. Note that porosity on sections is expressed by many porels, PORosity ELements. Porels can be identified by image analysis software by tracing porosity boundaries and identifying closed loops.

1). The porels might be produced by a few types, say $\mathcal{M}$, of three-dimensional objects e.g., *pore-types*. That is, the two-dimensional complexity arises from a few classes of pore-types, each pore-type yielding its representative collection of porels ranging in size and shape.

Ehrlich's image analysis procedure is designed to "deconvolve" the planar complexity into those more simple pore-types.

Derivation of pore-types relies on analysis of porosity of $\mathcal{K}$ binary images (for example, Figure 1).

The $\mathcal{K}$ binary images are quantified through erosion-dilation software in terms of $\mathcal{K}$ size and shape distributions (for example, Figure 2).

Those $\mathcal{K}$ size and shape distributions, so-called *smooth/rough spectra*, are the raw material of a pattern recognition/classification algorithm whose output consists of $\mathcal{M}$ pore-types expressed by $\mathcal{M}$ size and shape frequency distributions. Pore-types smooth/rough spectra are obtained by a two-fold polytopic vector analysis:

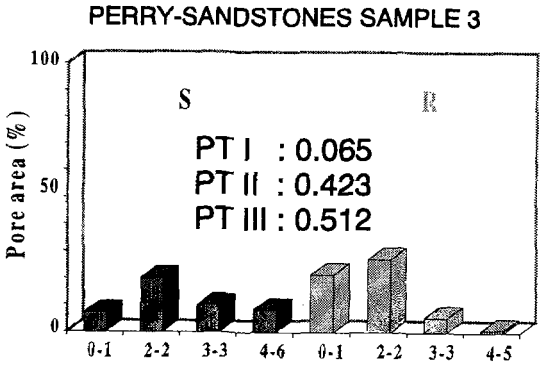

Figure 2. Smooth/Rough spectrum of Perry Sandstone sample 3 (Figure 1). The binary image displayed in Figure 1 is quantified by a smooth/rough spectrum obtained through erosion-dilation procedures. Each porel undergoes progressive degree of erosions followed by an equal degree of dilations. An erosion of degree i strips a porel of its i outermost strata of pixels; a dilation of degree i adds i strata of pixels to the porel. As erosion-dilation cycles go on, the porel is accordingly smoothed. The number of pixels lost between successive erosion-dilation cycles are recorded as a characteristic frequency distribution of roughness. The process is stopped as the number of erosions exceeds half the maximum width of the porel. Next-to-last dilation provides the smooth component of the porel. The binary image rough/smooth spectrum is formed by pooling all porel smooth/rough spectra and by converting pixels frequencies to proportions. Dark bars show the smooth (S) component, light bars the rough (R) component. Horizontal axes show class intervals of a frequency distribution calibrated in *units of length*. For example, for a pixel size of 15.44 μm, a smooth bin of boundaries **4–6** concerns a smooth seed of length-scales ranging from $((2 \times \mathbf{4}) - 1) \times 15.44$ μm to $(2 \times \mathbf{6}) \times 15.44$ μm, that is, from 108.08 μm to 185.28 μm.

- a dimensionality phase that involves Q- and R-mode principal component factor analyses to assess the minimum number, $\mathcal{M}$, of pore-types required to account for much of the variability of the k smooth/rough spectra,
- a polytope phase that builds a "simplex" enclosing the k smooth/rough spectra, with as many vertices e.g., pore-types smooth/rough spectra as derived by the dimensionality phase.

Space does not allow fuller discussion of that topic. Detailed account can be found in the literature (Miesch, 1976).

Ehrlich's pore-typing procedure (1991a) supplies as well, the size, the shape and the relative abundances $Np_{i,i=1,\mathcal{M}}$ within each binary image for all $\mathcal{M}$ pore-types.

In terms of Equation (2), the set of *geometrical* parameters, $\mathcal{P}^i_{i=1,\mathcal{M}}$, held to quantify the micro-geometry is:

$$(\mathcal{P}^i)_{i=1,\mathcal{M}} = (\text{pore-type}^i, Np_i)_{i=1,\mathcal{M}} \tag{13}$$

That geometrical set $\mathcal{P}^i_{i=1,\mathcal{M}}$ relates to the *sole* geometry of individual porels. Neither information about throats (two-dimensional surfaces lying in the plane of local narrowest constriction between two three-dimensional pores), nor information about the spatial correlation of the porels is contained in those $\mathcal{P}^i_{i=1,\mathcal{M}}$. In this

respect, Equation (13) *is not a complete measure of the three-dimensional micro-geometry*. The missing structural information is supplied by an implicit approach combining two-dimensional image analysis data e.g., $\mathcal{M}$ pore types, with three-dimensional data of petrophysical type e.g., mercury drainage experiments carried out on the same samples. A set of regression equations is derived, predicting the relative filling of each pore-type versus capillary pressure (P_c) (McCreesh *et al.*, 1991). In sandstones, the tendency of pore-types to fill in mutually exclusive and narrow ranges of P_c is a consequence of pores of like type to be mutually adjacent, connected by similarly-sized throats, *as an inescapable consequence of depositional processes* (Prince *et al.*, 1995).

The revealed association between pore-types and throat sizes $d_{j,j=1,\mathcal{M}}$ allows the use of a tube-like model (Equation (9)) to relate the functionals of the micro-geometry $Q^j_{j=1,\mathcal{M}} = (Np_j, d_j)_{j=1,\mathcal{M}}$ to k.

3. Predicting the Permeability Tensor of Natural Porous Media by the Local Change of Scale Method

The approach discussed above is a major advance in linking geometrical characteristics e.g., pore-types, to flow through natural media.

On the one hand, the nice feature of that approach is that the model (Equation (9)) arises from a revealed association between pore-types and throat sizes. On the other hand, the model produces the essential drawbacks peculiar to implicit approaches:

- lack of predictive character through a dependence on a set of samples ("tuning" constant C_k),
- lack of generality: applicability to limited rock-types: sandstones, carbonates.

The explicit approach discussed below aims at overcoming those drawbacks. The local change of scale method (Whitaker, 1986) leads, from first principles, to the macroscopic Darcy's law, spatially averaged over a local Representative Elementary Volume (R.E.V.) of Darcy's type noted $V_\beta(r_0)$. That technique yields furthermore a Stokes-like closure problem set at the microscopic scale over $V_\beta(r_0)$.

The form of the closure problem shows that *knowledge of the three-dimensional micro-geometry* allows explicit calculation of $\mathbf{K}$ as an implicit function of the micro-geometry.

Relevance of the local change of scale technique requires availability of three-dimensional micro-geometries. Three-dimensional micro-geometries cannot be obtained *directly* by current two-dimensional image analysis devices. A four-fold procedure is developed:

(1) *complete* characterization of the three-dimensional micro-structure of natural media by a set of N geometrical parameters $P^i_{i=1,N}$, derived by image analysis from a *single sample* (Equation (2)),

(2) assessment of a *minimum* and flow-relevant subset, $P^i_{i=1,N',N'\leq N}$ included in the complete measure $P^i_{i=1,N}$ (Equations (3) and (4)),

(3) use of that subset $P^i_{i=1,N'}$ to constrain a random stationary ergodic process allowing creation of three-dimensional synthetic media. This is the interface between the two-dimensional knowledge one has of porosity by image analysis ($P^i_{i=1,N'}$) and three-dimensional numerical implementations of the local change of scale technique (Anguy *et al.*, 1994a),

(4) formulation of a predictive analytical model capitalizing on relations of type Equation (4).

This paper focuses mainly on the geometrical aspects of the model.

3.1. Complete Characterization of the Micro-Geometry by Image Analysis

Image analysis is the method used to obtain micro-structural information from binary images. In the field of stereology, the two-dimensional relevance to the three-dimensional system only holds under either of two conditions: (1) isotropy of the micro-geometry, (2) existence of a single direction of anisotropy e.g., statistical axisymmetry (statistical invariance of the micro-geometry in planes rotating about that direction of anisotropy).

To a first approximation, statistical axisymmetry can be assumed in sandstones. This has been shown by strong correlations between two-dimensional characteristics, pore-types, measured in the plane perpendicular to bedding and physical properties measured on associated samples including: permeability, formation factor, mercury porosimetry (Ehrlich *et al.*, 1991a–b; McCreesh *et al.*, 1991).

Image analysis coupled with pattern recognition procedures revealed that isotropy in sandstones is rare at scales larger than mean grain size (l_σ) or mean pore size (l_β) due to the dynamics of the sedimentary processes. Intuitively, one will require a complete measure of the micro-geometry ($P^i_{i=1,N}$) to be assessed at some scale r_0 over a local geometrical R.E.V. ($V_\beta(r_0)$). $V_\beta(r_0)$ is a minimal volume comprising all geometrical characteristics of the macroscopic medium, large enough to avoid interactions between sampling and micro-structure and small enough to have bearing on the micro-geometry of a larger volume of practical interest. The size r_0 of $V_\beta(r_0)$ is that size at which *stationarity and ergodicity* of the micro-geometry can be declared. Two-dimensional Fourier-transforms of binary images yield:

- *quantitative* assessment of the characteristic length-scales of the spatial arrangement of porosity,
- *quantitative* assessment of that scale r_0 at which stationarity and ergodicity are met,
- *qualitative* display of the nature of the spatial complexity,

Capitalizing on statistical axisymmetry in sandstones, the geometrical parameters listed thereunder is held as a *complete* measure of the micro-structure. Thus;

$$(P^i)_{i=1,3} = (\epsilon_\beta, F(\nu_x, \nu_y), \zeta(\nu_x, \nu_y)) \tag{14}$$

where $F(\nu_x, \nu_y)$ is the Fourier modulus of the binary image, ν_x and ν_y wave-numbers along Cartesian axes, $\zeta(\nu_x, \nu_y)$ is a part of the complete Fourier phase $\varphi(\nu_x, \nu_y)$ (basic properties of Fourier transforms indicate that part of $\varphi(\nu_x, \nu_y)$ is not relevant).

The above set, $P^i_{i=1,3}$, is a complete measure since there exists, in two dimensions, a one-to-one transformation between the binary image and $(\epsilon_\beta, F(\nu_x, \nu_y), \zeta(\nu_x, \nu_y))$ to within trivial ambiguities (translation of the image, twin images).

3.2. Reducing the Geometrical Information

It is likely that the overall micro-geometry is not **K**-relevant. The complete measure determined above might be reduced to a simpler **K**-relevant subset, $P^i_{i=1,N',N'\leq 3}$. Along with other authors (Quiblier, 1984), phase-like information $\zeta(\nu_x, \nu_y)$ is assumed to contain no fundamental **K**-relevant structural information. The squared Fourier modulus $|F_e(\nu_x, \nu_y)|^2$ and its associated density probability function ϵ_β (e.g., porosity for a binary image) are held as a minimum **K**-relevant subset $P^i_{i=1,2}$. Equation (3) yields:

$$\mathbf{K} = g(\epsilon_\beta, |F_e(\nu_x, \nu_y)|^2) \tag{15}$$

The subscript "e" indicates that the micro-geometry has been "zero-appended" to derive $|F_e(\nu_x, \nu_y)|^2$ so that, based on the discrete form of the convolution theorem, either of $|F_e(\nu_x, \nu_y)|^2$ or a two-dimensional autocorrelation function $r(\lambda_x, \lambda_y)$ can be used. That is, $|F_e(\nu_x, \nu_y)|^2$ and $r(\lambda_x, \lambda_y)$ carry the *same* geometrical information. Thus;

$$\mathbf{K} = g(\epsilon_\beta, r(\lambda_x, \lambda_y)) \tag{16}$$

where λ_x and λ_y are wave-lengths in a Cartesian basis.

3.3. Random Stationary Ergodic Process

The two-dimensional nature of the micro-structure characterization $(P^i_{i=1,2} = (\epsilon_\beta, r(\lambda_x, \lambda_y))$ requires an *ad hoc* procedure to obtain three-dimensional micro-geometries. Such a procedure can be developed, treating the micro-structure as the realization of a *stationary ergodic* process characterized by its average ϵ_β and two-dimensional autocorrelation function $r(\lambda_x, \lambda_y)$.

Stationarity and ergodicity ensure that sample support problems are minimized (Anguy *et al.*, 1994b). Stationarity is commonly admitted for porous media "...

stationarity *would appear to be borne out by observation ...*" (Quiblier, 1984). Herein, stationarity is considered to stem from ergodicity. Ergodicity is declared from the non-splitting of the random process into elementary processes appearing with different probabilities (Ventzel, 1973). That is, ergodicity is declared if:

$$\lim_{\lambda_x, \lambda_y \to \text{image size}} r(\lambda_x, \lambda_x) \approx 0 \tag{17}$$

Within that framework, a random stationary ergodic process has been developed that yields a set of n two-dimensional and/or three-dimensional synthetic media, all characterized by measured ϵ_β and $r(\lambda_x, \lambda_y)$. A detailed account of the process would not fit this paper. The outline of this topic can be found, for example, in Joshi (1979). Qualitatively, the n synthetic media are derived convolving ϵ_β and $r(\lambda_x, \lambda_y)$ with Gaussian fields in a way similar to that of Gujar (1967), a pioneer in generating random sequences with averages and autocorrelation functions.

3.4. Direct Approach

The question is: are these synthetic media realistic? That is, does one capture in ϵ_β and $r(\lambda_x, \lambda_y)$ the essential characteristics of the micro-structure relevant to $\mathbf{K}$?

That raises the need of objective criteria to quantify the amount of information carried by ϵ_β and $r(\lambda_x, \lambda_y)$. This problem has been addressed in crystallography and optics as the so-called phase retrieval problem that concerns the uniqueness of the reconstruction of an object from $r(\lambda_x, \lambda_y)$. On the one hand, theoretical work, capitalizing on essential irreducibility of the z-transform of an object in more than one dimension yields that a unique object can be reconstructed from $r(\lambda_x, \lambda_y)$ (to within a few ambiguities) (Hayes, 1982). If so, the set $(\epsilon_\beta, r(\lambda_x, \lambda_y))$ fitted in the random process could be further reduced. On the other hand, other work, tackling the phase retrieval problem as a convolution problem showed that $r(\lambda_x, \lambda_y)$ yields a large number of admissible geometries (Brames, 1987). Hence the requirement to quantify information comprised of ϵ_β and $r(\lambda_x, \lambda_y)$.

In this respect, the direct method outlined at the beginning of Section 3 can be used. If all $\mathbf{K}$-relevant structural information is carried by ϵ_β and $r(\lambda_x, \lambda_y)$ then, n synthetic media generated from single set $(\epsilon_\beta, r(\lambda_x, \lambda_y))$ must yield n permeability tensors $\mathbf{K}^i_{i=1,n}$ such that:

$$\mathbf{K}^1 \approx \mathbf{K}^2 \approx \mathbf{K}^3 \approx \cdots \approx \mathbf{K}^n \tag{18}$$

where, $\mathbf{K}^i_{i=1,n}$ are calculated numerically by the local change of scale technique. Furthermore, the $\mathbf{K}^i_{i=1,n}$ must be consistent with some experimental measure of the permeability $k^{\text{experimental}}$.

A test has been performed in two-dimensions. A set of n synthetic media were derived from artificial set $(\epsilon_\beta, r(\lambda_x, \lambda_y))$:

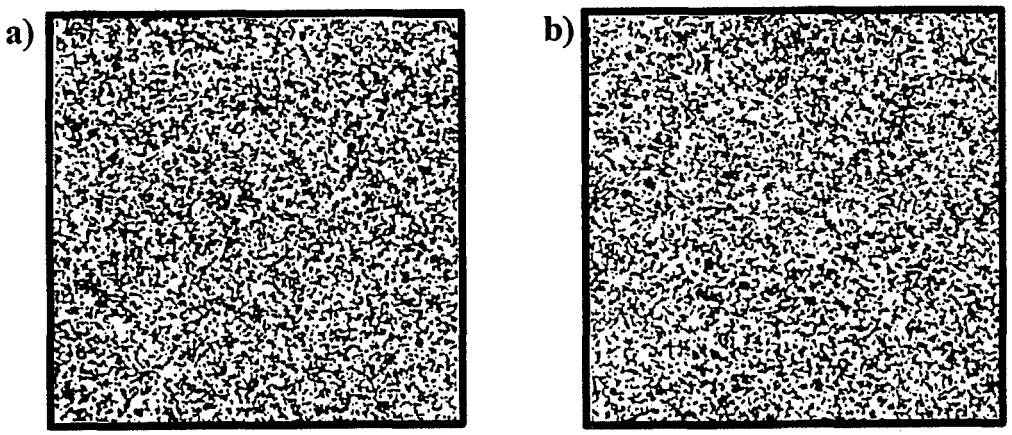

Figure 3. (a) and (b): examples of two artificial isotropic media of size ($50x r_0 \times 50x r_0$) generated by a random stationary ergodic process constrained by the same average and isotropic autocorrelation function. Porosity expressed by white.

- $\epsilon_\beta = 60\%$,
- $r(\lambda_x, \lambda_y)$ is isotropic and equal to zero for all λ_x and λ_y such that $(\lambda_x^2 + \lambda_y^2)^{1/2} \geq 8$ pixels. That is, the local geometrical R.E.V. $V_\beta(r_0)$ is achieved at that scale $r_0 = 8$ pixels at which the micro-geometry is stationary ergodic.

The local change of scale method operates over a local R.E.V. of Darcy's type, $V_\beta(r_0)$, treated as a unit cell in a spatially periodic porous media so that the periodic assumption is implicit to the local change of scale method. $V_\beta(r_0)$ must contain enough $V_\beta(r_0)$ for random effects to be faithfully accounted for. In the *particular case* treated here, the additional effects produced by the periodic boundary condition imposed at the limits of $V_\beta(r_0)$ have been quantified (Bernard, 1995), showing that for *large enough* $V_\beta(r_0)$ (so as to account the required randomness at scale larger than $V_\beta(r_0)$), periodicity is a weak condition compared to dominant no-slip boundary condition imposed at the solid-fluid interface within the medium.

Two examples of such media, of size $50x r_0 \times 50x r_0$ are displayed as Figure 3. The curves in Figure 4 display results obtained by computing K by the local change of scale model using R.E.V.s of Darcy's type of increasing sizes and common centre.

This confirms that $V_\beta(r_0)$ must be larger than $V_\beta(r_0)$ for random effects to be accurately accounted for, such that;

$$r_0 \approx 30x r_0. \tag{19}$$

Convergence of the permeability tensors towards the same value ($\approx$50 Darcys) (Figure 4) is a *necessary* condition to ensure that (ϵ_β, $r(\lambda_x, \lambda_y)$) carry all K-relevant structural information. Similar results have been obtained for many other synthetic media derived from the parameters mentioned above.

Adler *et al.* (1990) attempted to apply a quite similar direct approach in three dimensions to Fontainebleau-sandstones. Discrepancies found by Adler *et al.*

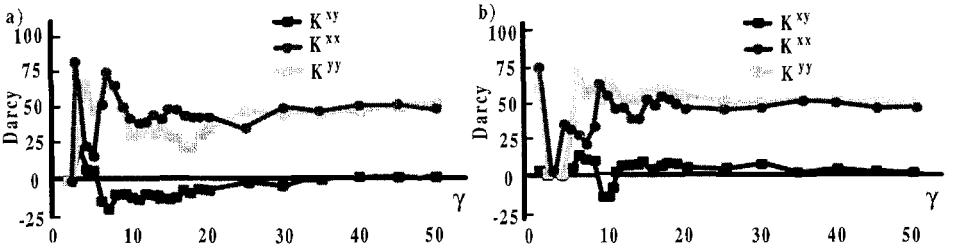

Figure 4. (a) and (b): numerical evolution of the permeability tensor K calculated by the local change of scale method as a function of the size of the local Darcy's R.E.V. ($V_\beta(r_0)$) for the synthetic isotropic media displayed in Figures 3a and 3b respectively. Horizontal axes calibrated in r_0 (characteristic length-scale of the local geometrical R.E.V.) (r_0 = 8 pixels) so that the size γ of $V_\beta(r_0)$ goes from r_0 to $50 x r_0$ (400 pixels).

(1990) between modelled and experimental permeabilities are likely to be due to several too restrictive assumptions: (1) use of an isotropic autocorrelation, (2) use of a too small Darcy's R.E.V. of size $r_0 \approx 3 x r_0$, likely to contribute significantly to the large variance characterizing the modelled permeabilities (random effects not faithfully accounted for), (3) use of a too small $V_\beta(r_0)$, $r_0 \sim 100$ μm ($\sim$ grain size) as support for measured ϵ_β and isotropic $r(\lambda_x, \lambda_y)$.

Indeed, recent work (Prince *et al.*, 1995; Anguy *et al.*, 1994b) showed that sandstones contain a universal structural hierarchy, mainly as a result of the depositional processes. The reasons for that were given in a paper by Graton *et al.* (1935). Sandstone micro-structure can be viewed as a domainal structure of juxtaposed well-packed grain-clusters bounded by packing-flaws. Flaws are zones of disorder formed through a variety of depositional processes discussed by Prince *et al.* (1995). Close- and loose-packed domains are the fundamental textural elements, a *first order structure* in a hierarchy. In ascending length-scales, the *second order structure* consists of loose-packed zones coalescing into circuits throughout a matrix of close-packed domains. *Third order structures* concern various modes of clustering of the loose-packed circuits as well as contrasts due to grain size.

As discussed further, work by Ehrlich *et al.* (1991b) bases the K-relevance of structural levels on the first and second orders. The K-relevance of third order structural levels remains unknown at present.

As a consequence, any attempt to prove that $(\epsilon_\beta, r(\lambda_x, \lambda_y))$ carries all K-relevant structural information, by verifying Equation (18), *must reproduce within the three-dimensional synthetic media those three structural levels.* Use of a correlation length of roughly 100 μm (that is $\sim (l_\sigma, l_\beta)$) invalidates the Adler *et al.* (1990) attempt wherein the first order structural level is not even faithfully accounted.

Commonly, structures of third order have length-scales, $\lambda^{\text{Clusters}}$ of the order of several cm (given a mean grain size $l_\sigma \sim 200$ μm). Even using a voxel size of 15 μm requires a three-dimensional synthetic medium consisting of several billions of

voxels. Therefore, due to present-day computational limitations, second and higher order structural levels cannot be simulated. So the permeability of the simulated medium cannot be compared with the permeability measured on the sample from which it was derived.

4. Indirect Tests on the Validity of Simulated Media: Results

However, the fidelity of the simulated medium can be assessed by comparing patterns of porosity exposed in sections through the simulated medium with those exposed on the actual prototypical samples. That is, the synthetic sections can be subjected to the same image analysis procedures (Ehrlich *et al.*, 1991a) as those derived from actual media. It has been demonstrated that, in general, correlations exist between pore-types and mercury injection curves (McCreesh *et al.*, 1991). Riggert (1994) verified this for the sandstones discussed in this paper. Thus if the simulated sections display the same pore-type proportions as the prototype samples and also display the networks of packing flaws upon which the correlation with mercury porosimetry is based, then the simulated media should have the same permeability as that of the sample that yielded both ϵ_β and $r(\lambda_x, \lambda_y)$.

Eleven binary mosaics of sandstones were used to derive pore-types using Ehrlich's image analysis software (Ehrlich *et al.*, 1991a). As an example, sample 3 is displayed in Figure 1. All samples come from four Pennsylvanian subsurface sand units including (Riggert, 1994):

- samples from the upper part of the Hoover Sandstones: medium- to fine-grained quartz arenite (samples 7 and 8), samples from the lower Hoover Sandstones: fine- to very fine-grained subarkose and sublitharenite (sample 1),
- samples from the Elgin Sandstones: fine- to very fine-grained quartz arenite and subarkose (sample 9),
- samples from the Perry Sandstones: fine-grained quartz arenite, subarkose, and sublitharenite (samples 2 to 4),
- samples from the Layton Sandstones: fine- to very fine-grained lithic subarkoses, subarkoses, and feldspathic litharenites (samples 5, 6, 10 and 11).

All samples come from the same well, drilled east of Newkirk, Kay County, Oklahoma, as part of an international consortium, the Conoco Borehole Test Project (C.B.T.P.), on a Conoco Production Research and Development initiative. Three pore types were derived to characterize the porels of the eleven samples. Smooth/rough spectra and petrographic appearance of the three pore-types are displayed in Figure 5. Proportions of each pore-type within the eleven samples are listed in Table I.

Synthetic two-dimensional slices have been generated, for sample 3 (Perry Sandstones) by the random process discussed in Section 3.3. Porosity ($\epsilon_\beta = 0.2089$)

Table I

Pore-type relative abundances in the 11 sandstone samples as derived by the Extended Q-Model of Ehrlich *et al.* (1991a)

	PTI relative abundance	PT II relative abundance	PT III relative abundance
Sample 1	0.1114	0.7793	0.1093
Sample 2	0.0388	0.4815	0.4796
Sample 3	0.0647	0.4235	0.5118
Sample 4	0.0000	0.7693	0.2307
Sample 5	0.4574	0.5426	0.0000
Sample 6	0.4828	0.5046	0.0126
Sample 7	0.0440	0.3017	0.6543
Sample 8	0.0946	0.0145	0.8909
Sample 9	0.2124	0.7164	0.0713
Sample 10	0.8902	0.0631	0.0468
Sample 11	0.9327	0.0194	0.0479

and two-dimensional autocorrelation function, $r(\lambda_x, \lambda_y)$ measured on sample 3 (Figure 1) were fitted in the random process. Of course, other values of ϵ_β and $r(\lambda_x, \lambda_y)$ would have to be used for simulating synthetic slices of the other sandstones listed in Table I. Only that part of $r(\lambda_x, \lambda_y)$ related to lags (λ_x, λ_y) verifying inequalities (20) is accounted for. That is, no spatial correlation is imposed within the synthetic media at scales larger than 478.7 μm.

$$|\lambda_x| \leq 478.7\ \mu\text{m and } |\lambda_y| \leq 478.7\mu\text{m} \tag{20}$$

This correlation length, $L_c = 478.7\ \mu$m, is consistent with:

- the mean length-scales of the porels derived from the three pore-types to be reproduced (29.0 μm, 43.7 μm and 62.5 μm respectively, as derived by Ehrlich's pore-typing procedure),
- the requirement by the random process for $r(\lambda_x, \lambda_y)$ to verify (Joshi, 1979):

$$\lim_{\lambda_x, \lambda_y \to L_c} r(\lambda_x, \lambda_y) \approx 0 \tag{21}$$

Over the lags accounted for (relations 20), $r(\lambda_x, \lambda_y)$ turned out not to depart significantly from an isotropic autocorrelation. In that respect an isotropic autocorrelation $r^{Is.}(\lambda_x, \lambda_y)$ has been fitted to the random process. Isotropy of the porosity over length-scales smaller than 478.7 μm ensures that the frequency distributions representing three-dimensional pore-types are unbiased as a consequence of the plane of section intersecting a large number of pores whose orientations and positions are random with respect to the plane of section. The synthetic media have been added, as external samples to Ehrlich's software and defined in terms of the pore-types

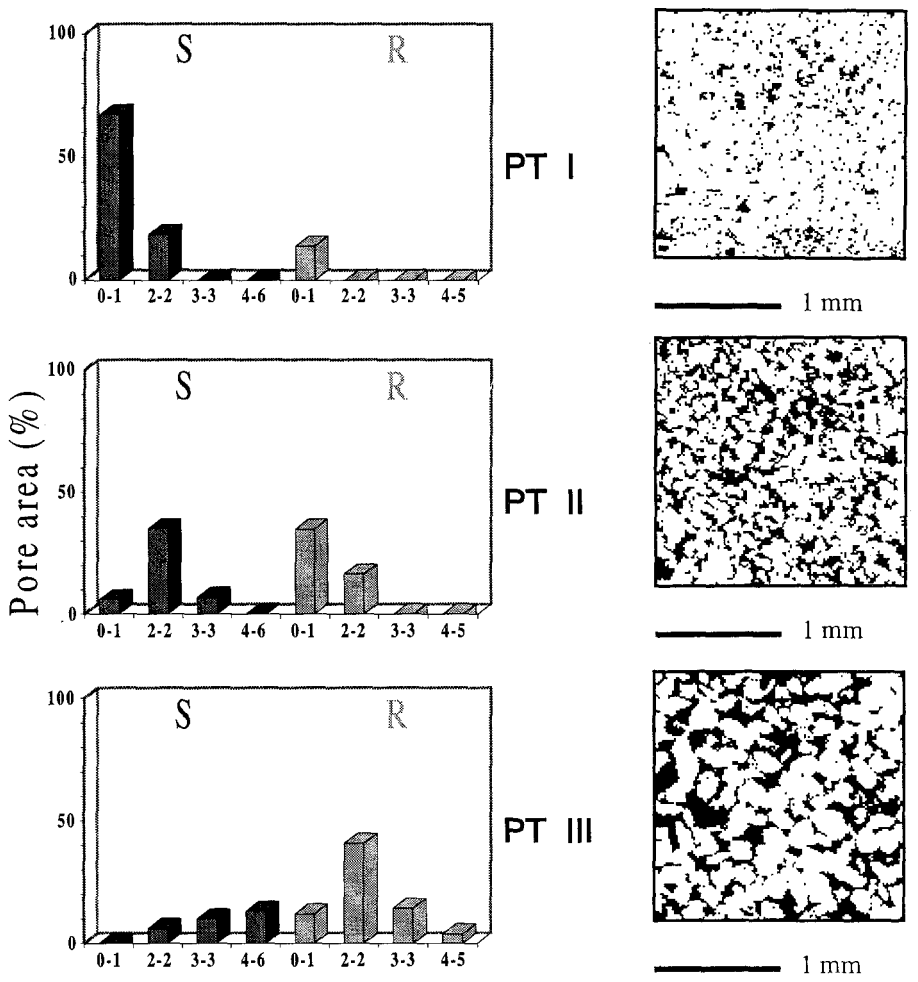

Figure 5. Smooth/rough spectra of the three pore types (PT) derived through Ehrlich's petrographic Image Analysis Software (Ehrlich et al., 1991a). The mean size of each pore type is calculated through the formula of the mean of grouped data. Mean sizes for PT I, PT II and PT III are 29.0 μm, 43.7 μm and 62.5 μm respectively as supplied by Ehrlich's software. Based on examination of Table I, the visual appearance of pore-types is straightforward by picking up sub-domains of samples having high relative proportions of a given pore-type.

obtained for the eleven C.B.T.P. sandstone samples. Achieved pore-type relative abundances for three of those synthetic samples are listed, as examples, in Table II. Synthetic sample 2 is displayed in Figure 6. Its associated smooth/rough spectrum, as derived by Ehrlich's procedure, is displayed in Figure 7.

Results listed in Table II yield two remarks: (1) all synthetic samples have, by-and-large, the same pore-type proportions, (2) the pore-type proportion agreement between real Perry-Sandstone sample-3 and the synthetic samples is quite good. This is a strong argument to state that the geometrical parameters $P^i_{i=1,2}$ =

Table II

Comparison of the pore-type relative abundances of 3 synthetic isotropic slices generated by a random stationary ergodic process constrained by porosity and isotropic autocorrelation function measured on sample 3

	PT I relative abundance	PT II relative abundance	PT III relative abundance
Sample 3	0.0647	0.4235	0.5118
Synthetic sample 1	0.1366	0.4238	0.4396
Synthetic sample 2	0.1369	0.4449	0.4181
Synthetic sample 3	0.1195	0.4306	0.4499

$(\epsilon_\beta, r^{Is\cdot}(\lambda_x,\lambda_y))$ carry pore-type-like information. That is, synthetic media derived in this work from sample 3 do have the first order structural level present in all sandstones. The same result has been obtained for all sand units discussed at the beginning of the current section. In brief, those results, obtained by merging two different approaches allow partial quantification of the nature of the geometrical information carried by $(\epsilon_\beta, r^{Is\cdot}(\lambda_x, \lambda_y))$.

5. Discussion

Work completed by the authors reveals that synthetic media generated through a random stationary ergodic process are rock-like, in terms of their pore-type content. Pore-types arise from the dynamics of depositional processes, yielding a universal first order structural level: a *domainal structure* consisting of efficiently packed clusters of grains bounded by loose-packed domains. That first order structural level can be *qualitatively* delineated by Fourier transform analysis as displayed in Figure 8. Both real (Figure 8a) and synthetic (Figure 8b) media show statistically similar first order structure represented by stippled pattern. Note that the stippled pattern selectively overlays porels in loose-packed domains derived from pore-types II and III.

Second order structure is displayed on Figure 9a and consists mainly of independent circuits of porels derived from pore-type III, and to a less extent, of circuits of porels derived from pore-type II. That is, the association between pore-types and throat sizes as predicted implicitly by Ehrlich *et al.* (1991a–b) and McCreesh *et al.* (1991) would be the same as that one displayed in Figure 9a. In this example, the characteristic length-scale of the circuits is $\lambda^{\text{Circuits}} = 494.1$ μm, as derived by Fourier analysis. That is, $\lambda^{\text{Circuits}}$ is of the same order as the imposed correlation length L_c ($L_c = 478.7$ μm). This, combined with the quite random spatial arrangement of the circuits (Figure 9a) yields a statistically analogous structural level of second order for both synthetic (Figure 9b) and natural media (Figure 9a). Figure 10a displays the third order structural level in the hierarchy (contrasts in

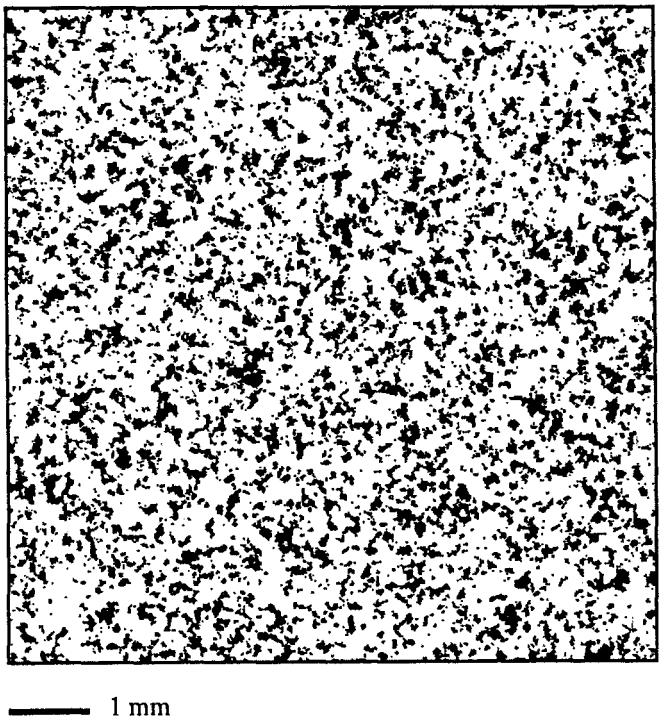

Figure 6. Isotropic synthetic sample 2 derived from ϵ_β, $r^{Is.}(\lambda_x, \lambda_y)$ measured on Perry-sandstone sample 3 (Figure 1). Image Size: 7.905 mm × 7.905 mm (512 × 512 pixels, square pixel edge: 15.44 μm). Image is random at scales larger imposed correlation length L_c = 478.64 μm (31 pixels). Porosity represented by black.

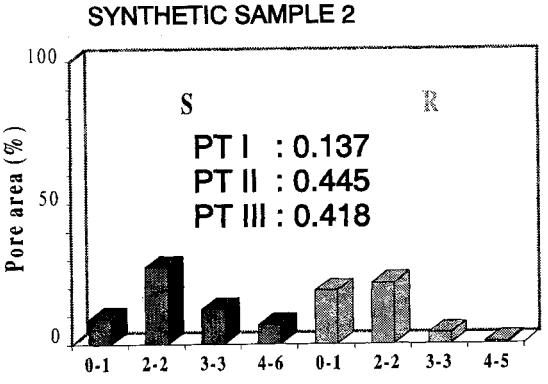

Figure 7. Smooth/rough spectrum of synthetic sample 2 (Figure 6) (See caption of Figure 2 for details).

porosity due to a particular mode of clustering of the circuits displayed on Figure 9a). This level, of length-scale, $\lambda^{\text{Clusters}}$ = 1317.6 μm, appears quite random in

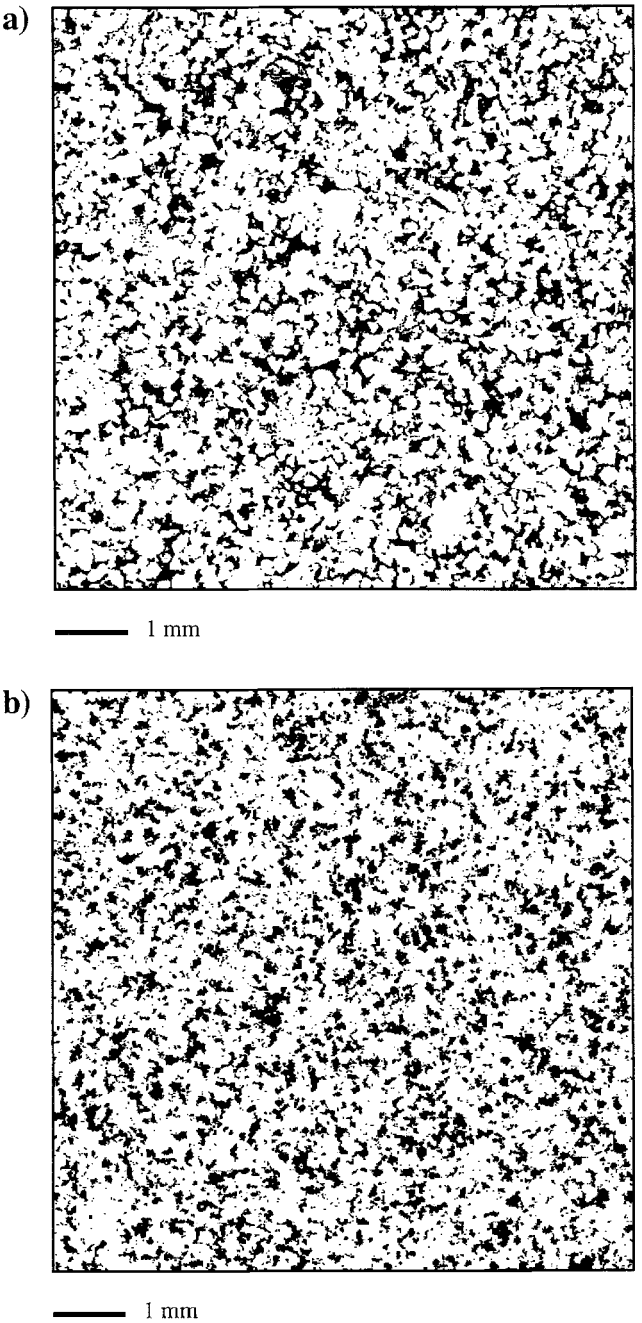

Figure 8. Filtered reconstructions for, (a) Perry-Sandstone sample 3 and (b) synthetic sample 2. Stippled pattern represents image after filtering all wave-lengths smaller or equal to grain size ($\sim$231.0 μm). Original images expressed by black representing porosity. In both real and synthetic cases, the stippled pattern selectively overlays oversized pores associated with packing flaws, the lowest structural level in a hierarchy. The achieved displays of structural heterogeneities are only qualitative in that: (1) the cutoff value used to binarize the filtered images is not universal, (2) Fourier filtering concerns only the *size* of the heterogeneities and not their shape.

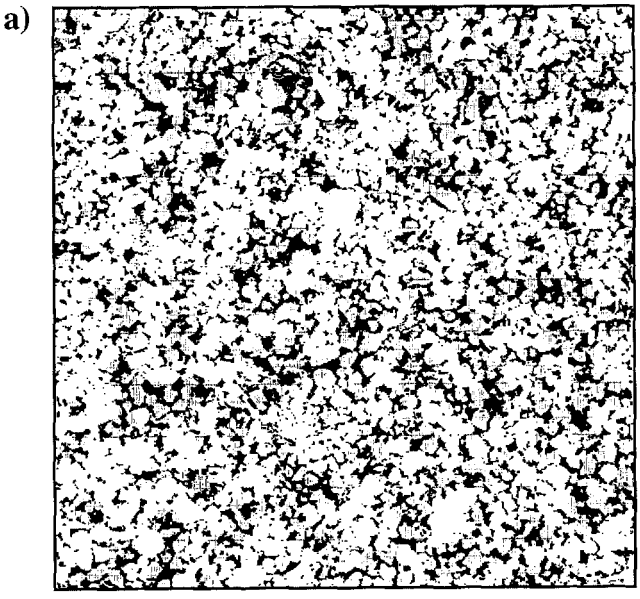

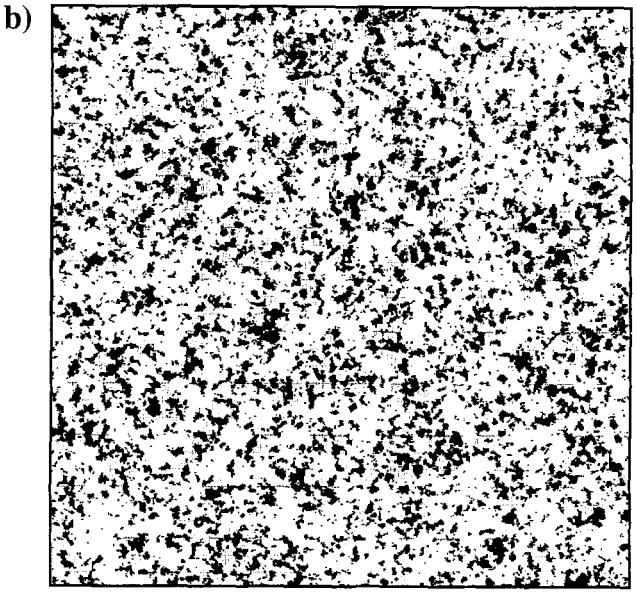

Figure 9. Similar to Figure 8 except filtered at wave-length 494.1 μm, revealing complete circuits of packing flaws.

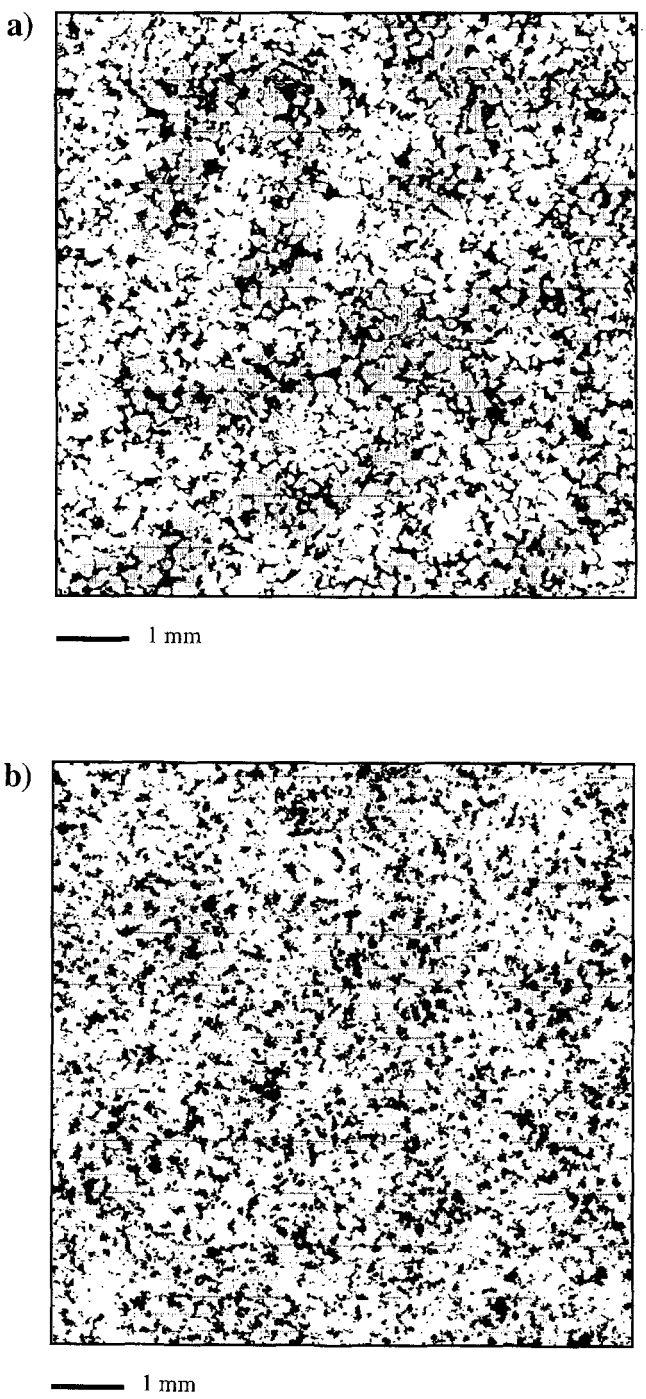

Figure 10. Similar to Figure 8 except filtered at wave-length 1317.6 μm, revealing a higher level in a structural hierarchy.

Perry-Sandstone sample 3 (Figure 10a). Again there is statistical similarity with synthetic sample 2 (Figure 10b), *random* at scales larger than L_c.

Commonly, sandstones are more structured, with larger $\lambda^{\text{Circuits}}$ and $\lambda^{\text{Clusters}}$. Furthermore, at scales of the order of $\lambda^{\text{Circuits}}$, sandstones are commonly *anisotropic*. That is, anisotropic $r(\lambda_x, \lambda_y)$ with correlation lengths of a *few cm* must be fitted in the random process to reproduce the complete hierarchy of structures.

As mentioned above, this is impractical using the current random process. A new simulation is currently being developed by the authors, allowing reproduction of the complete structure. The debate whether or not all structural components in sandstones must be reproduced to generate **K**-relevant synthetic media will then be addressed through a two-fold procedure:

- compare filtered binary sandstone images (of type Figures 8a, 9a, 10a) with filtered slices through three-dimensional synthetic media,
- compare mercury porosimetry curves obtained on natural samples with *numerical* mercury drainage experiments carried over three-dimensional synthetic media comprising structural levels up to second order and up to third order. This mercury drainage numerical simulator is currently developed.

Acknowledgments

The authors would like to extend their thanks to Dr. J. B. Ferm, Vice President of Perception & Decision Systems Inc. (P.A.D.S.) for graciously providing a Petrographic Image Analysis System (P.I.A.S.) and for numerous and valuable instructions for use of P.I.A.S. The authors would also like to thank Dr. Paul W. J. Glover and the reviewers for allowing the authors to contribute to this Special Issue of *Surveys in Geophysics*. The authors would also like to thank Dr. V. L. Riggert for supplying the binary images presented in this work. The authors are grateful to the CNRS Research Group, T.R.A.B.A.S., for financial support.

References

Adler, P. M., Jacquin, C. G. and Quiblier, J. A.: 1990, 'Flow in Simulated Porous Media', *Int. J. Multiphase Flow* **16**(4), 691–712.

Anguy, Y., Bernard, D. and Ehrlich, R.: 1994a, 'The Local Volume Averaging Technique for Modelling Flow in Natural Porous Media (1): Numerical Tools', *Advances in Water Resour.* **17**, 337–351.

Anguy, Y., Ehrlich, R., Prince, C. M., Riggert, V. and Bernard, D.: 1994b, 'The Sample Support Problem for Permeability Assessment in Reservoir Sandstones', in J. M. Yarus and R. L. Chambers (eds.), *A.A.P.G. Computer Applications in Geology No. 3*, pp. 37–54.

Anguy, Y.: 1993, *Application de la Prise de Moyenne Volumique à l'Etude de la Relation entre le Tenseur de Perméabilité et la Microgéométrie des Milieux Poreux Naturels*, thèse Univ. Bordeaux 1, 170 pp.

Azam, M. I. S. and Dullien, F. A. J.: 1977, 'Flow in Tubes with Periodic Step Changes in Diameter: A Numerical Solution', *Chem. Eng. Sci.* **32**, 1445–1555.

Bernard, D., 1995, 'Using the Volume Averaging Technique to Perform the First Change of Scale for Natural Random Porous Media', in G. Gambolati (ed.), *Advanced Methods for Groundwater Pollution Control,* Springer Verlag, New York, pp. 9–18.

Brames, B. J.: 1987, 'Efficient Methods of Support Reduction', *Opt. Commun.* **64**, 333–337.

Bryant, S. L., King, P. R. and Mellor, D. W.: 1993, 'Network Model Evaluation of Permeability and Spatial Correlation in a Real Random Sphere Packing', *T.i.P.M.* **11**, 53–70.

Chatzis, I. and Dullien, F. A. J.: 1977, 'Modelling Pore Structure by 2-D and 3-D Networks with Application to Sandstones', *J. Canad. Pet. Techno.* **16**, 97–108.

Dullien, F. A. J.: 1979, *Porous Media: Fluid Transport and Pore Structure,* New York, Academic Press, 396 p.

Dullien, F. A. J.: 1975, 'New Network Permeability Model of Porous Media', *A.I.Ch.E. J.* **21**(2), 299–307.

Ehrlich, R., Crabtree, S. J., Horkowitz, K. O. and Horkowitz, J. P.: 1991a, 'Petrography and Reservoir Physics I: Objective Classification of Reservoir Porosity', *A.A.P.G. Bulletin* **75**(10), 1547–1562.

Ehrlich, R., Etris, E. L., Brumfield, D., Yan, L. P. and Crabtree, S. J.: 1991b, 'Petrography and Reservoir Physics III: Physical Models for Permeability and Formation Factor', *A.A.P.G. Bulletin* **75**(10), 1579–1592.

Garboczi, E. J.: 1990, 'Permeability, Diffusivity and Micro-Structural Parameters: A Critical Review', *Cement and Concrete Research* **20**, 591–601.

Graton, L. C. and Fraser, H. J.: 1935, 'Systematic Packing of Spheres with Particular Relation to Porosity and Permeability', *J. Geology* **43**(8), 785–909.

Gujar, U. G.: 1967, *Generation of Random Signals with Specified Probability Density Functions and Power Density Spectra,* M.Sc.E. thesis, Dept. of Elec. Engng., Univ. of New Brunswick, Fredriction, N.B., Canada.

Haring, R. E. and Greenkorn, R. A.: 1970, 'Statistical Models of Porous Medium with Non-Uniform Pores', *A.i.Ch.E. J.* **16**(3), p. 477.

Hayes, M. H. and McClellan: 1982, 'Reducible Polynomials in More than One Variable', *Proc. I.E.E.E.* **70**, 197–198.

Joshi, M. Y.: 1979, *A Class of Stochastic Models for Porous Media,* Ph.D. Dissertation, Engng. Petroleum, Univ. of Kansas, 154 pp.

McCreesh, C. A., Ehrlich, R. and Crabtree, S. J.: 1991, 'Petrography and Reservoir Physics II: Relating Thin Section Porosity to Capillary Pressure, the Association between Pore Types and Throat Sizes', *A.A.P.G. Bulletin* **75**(10), 1563–1578.

Miesch, A. T.: 1976, 'Q-Mode Factor Analysis of Geochemical and Petrologic Data Matrices with Constant Row Sums', U.S. Geol. Surv. Prof. Pap., 574-G, 47 pp.

Prince, C. M., Ehrlich, R. and Anguy, Y.: 1995, 'Analysis of Spatial Order in Sandstones II: Grain Clusters, Packing Flaws and the Small-Scale Structure of Sandstones', *J. of Sed. Research* **A65**(1), 13–28.

Quiblier, J. A.: 1984, 'A New Three-Dimensional Modeling Technique for Studying Porous Media', *J. of Colloid and Interface Sci.* **98**(1), 84–101.

Riggert, V. L.: 1994, *Petrophysical Relationships of Pores and Pore Throats to Spatial Fabric Elements in Sandstones and their Implications for Fluid and Electrical Flow,* Ph.D. thesis, Univ. of South Carolina, 192 pp.

Scheidegger, A. E.: 1974, *The Physics of Flow Through Porous Media*, University of Toronto Press, 353 pp.

Thompson, A. H.: 1991, 'Fractals in Rock Physics', *Annu. Rev. Earth Planet Sci.* **19**, 237–262.

Ventzel, H.: 1973, *Théorie des Probabilités,* eds. Mir Moscou, 584 pp.

Whitaker, S.: 1986, 'Flow in Porous Media 1: A Theoretical Derivation of Darcy's Law', *T.i.P.M* **1**, 3–25.